DOI: 10.1021/ma102243u

Macromolecules
ARTICLE

Intrinsic Fluorescence Studies of Conformational Relaxation and Its Dynamics of Triblock Copolymer during the Micellization in Selective Solvents

Jin Yang,[†] Xindan Zheng,[†] Bin Zhang,[‡] Ruowen Fu,[‡] and Xudong Chen*,[†]

[†]*Institute of Polymer Science, DSAPM Lab, OFCM Institute, School of Chemistry and Chemical Engineering, Sun Yat-Sen University, Guangzhou 510275, P. R. China, and* [‡]*Key Laboratory for Polymeric Composite and Functional Materials of Ministry of Education, School of Chemistry and Chemical Engineering, Sun Yat-sen University, Guangzhou 510275, P. R. China*

Received September 29, 2010; Revised Manuscript Received January 5, 2011

ABSTRACT: The aggregation behaviors of an ABA block copolymer, polystyrene-*b*-poly(ethylene/butylene)-*b*-polystyrene triblock copolymer (SEBS), were investigated in methylene dichloride (selective solvent for PS block) and mixture of *n*-hexane and cyclohexane (selective solvent of PEB block), i.e., SEBS-(S) and SEBS-(EB) solution, respectively. Both static and dynamic light scattering showed that the conformational change of molecular chain underwent three stages in SEBS-(S) solution. By using steady-state and time-resolved fluorescence, it was concluded that, when the micellization process of SEBS-(S) solution occurred, PS segments was dramatically stretched during the aggregation of PEB block into micelle cores, resulting in the great decrease in the amount of intramolecular excimers. In the case of SEBS-(EB) solution, five stages were observed in dynamic light scattering result during the micellization, suggesting that further aggregation between micelles was induced by the bridging effect of the dangling outer block (PS). The steady-state fluorescence results indicated that the intermicellar aggregation would not lead to a dramatic decrease in interchain distance of PS block in micelle cores. Interestingly, the time-resolved fluorescence indicated that, for SEBS solutions, the conformation of PS block was completely homogeneous in its selective solvent but microheterogenous in the solvent selective for PEB block. Moreover, the activation energy of excimer association and dissociation in both SEBS solutions were also estimated, which can be considered as the key parameters for characterizing the comformation of macromolecular chains during the micellization process.

Introduction

The aggregation behaviors of block copolymers have at tracted intense interest in both the academic and industrial communities due to their unique physical properties during past three decades.[1−4] Much of this attention has been concerned with AB and ABA block copolymers in selective solvents, i.e., a thermodynamically good solvent for one block and precipitant for the other block.

It is well recognized that, for ABA triblock copolymers in selective solvents for the outer blocks, the micellization process obeys the close association mechanism, which assumes a dynamic equilibrium between the copolymer chain and micelles with a certain association number.[5] However, the association behavior of triblock copolymers in selective solvents for the middle block is much more complex since various factors can influence the micellization process and the structural parameters of micelles, including composition, structure, molar mass of the copolymer, interactions between the copolymer blocks and the solvent, copolymer concentration, temperature, etc.[6−9] For example, flowerlike micelles can be formed if the middle block forms a loop and both outer blocks stay in the micelle core. In addition, the existence of branched structures at low concentrations or gel-like networks at high enough concentrations would also be possible due to a bridging function of the soluble middle blocks extended between the small clusters formed by the outer blocks. Note that, although a large number of investigations have been carried out to characterize the micelle structure, few of them have paid attention to the conformational change at the interface of two blocks, the inner structure of micellar aggregates, etc.

From one experimental point of view, the molecular level information on polymer chain motions will redound to the understanding of the correlation between microstructure and interaction of micelles. So far, the aggregation behaviors of micelles from block copolymers have been mainly studied by several scattering techniques, such as static laser light scattering (LLS),[10] dynamic light scattering (DLS),[11] small-angle neutron scattering (SANS),[12] etc. Actually, during the past years, fluorescence spectroscopy has been proven to be a very sensitive method in studying aggregation and phase separation behavior at the molecular level.[13−15] The fluorescence method can provide information on a scale smaller than conventional light scattering and comparable to SANS.[16] However, the labeling procedure is often tedious. More importantly, in most of the fluorimetric studies of polymer, the fluorescent probe was covalently attached to one of the polymers, which in fact changed the microenvironment of macromolecules and made the macromolecules more hydrophobic, thus enhancing their complexation ability. It is worth mentioning that, without any probe and labeling, the intrinsic fluorescence emission was also highly sensitive to issues ranging from local polymer conformational populations in solution and phase behavior in polymer blends to local microenvironments in bulk homopolymers.[17−21]

In our previous researches,[22,23] the intrinsic fluorescence spectra were found to be very simple and sensitive means to

*Corresponding author: e-mail cescxd@mail.sysu.edu.cn; phone +86-20-84113498.

 Published on Web 01/27/2011

Scheme 1. Chemical Structure of SEBS[a]

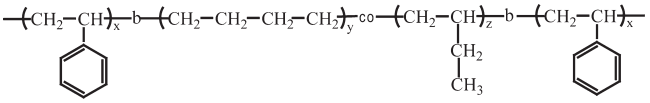

[a] x and $y + z$ stand for the polymerization degrees of the PS and PEB blocks, respectively.

characterize the transition of molecular conformation and aggregation of macromolecular chains. Herein, the intrinsic fluorescence methods were used to study conformational changes and association behavior of a model polymer, i.e., polystyrene−poly(ethylene/butylene)-*b*-polystyrene triblock copolymer (SEBS), which is known to form interesting core−shell micelles in several solvents.[24−26] The intra- and intermacromolecular interactions in response to temperature in selective solvent were probed by steady-state and time-resolve fluorescence. In addition, to obtain deeper understanding, the light scattering method was also applied to further elucidate the kinetics and detailed mechanism of the micellar self-assembly of SEBS in selective solvents. It is hoped the obtained result should be able to improve our understanding of the aggregation of ABA copolymers in selective solvents.

Experimental Section

Materials and Solution Preparation. SEBS (Kraton G1650, $M_w = 1.73 \times 10^5$, PDI = 1.12, styrene content 29 wt %) purchased from Shell Development Co. was purified by dissolution in toluene and precipitation in methanol at least three times. The chemical structure is shown in Scheme 1. All solvents (analytical reagent) were purchased from Guangzhou Chemical Reagent Factory (Guangzhou, China) and used without additional purification. In this experiment, two types of solutions, SEBS(S) and SEBS(EB), were obtained by dissolving a known amount of copolymer in the solvent selective for PS block (methylene dichloride) and for PEB block (mixture of *n*-hexane and cyclohexane), respectively. To satisfy the requirement of our instrument, the molar ratio of hexane/cyclohexane is 3.6/1, and the concentration of SEBS solution is 1.2×10^{-3} g/mL unless otherwise indicated.

Methods. The static light scattering (SLS) signal was collected with a FLS920 combined fluorescence lifetime and steady state spectrometer (Edinburgh, UK) at a cooling rate of 1 K/min. Both excitation and emission monochromator wavelengths were 500 nm. This spectrophotometer possesses a single-cell Peltier holder, which is an electronically controlled thermostat single-cell accessory capable of controlling the temperature to within ±0.1 K.

Dynamic light scattering (DLS) measurements were conducted on a Brookhaven BI-200SM apparatus with a BI-9000AT digital correlator and a He−Ne laser at 532 nm. Prior to the measurement, the sample solutions were filtered through nylon filters (13-HV, Millipore, 0.45 μm pore size). The data were analyzed by the CONTIN algorithm, while the hydrodynamic radius (R_h) and size polydispersity of the micelles were obtained by a cumulant analysis of the experimental correlation function.

Both steady-state and time-resolved fluorescence were also recorded with the aforesaid fluorescence spectrophotometer. In steady-state measurement, the slit (ex/em) width of the measurements was 1.5 nm/2.5 nm. As for time-resolved measurement, the excitation was carried out by a pulsed hydrogen flash lamp controlled by a thyratron tube operating with a repetition frequency rate of 40 kHz. For a lifetime analysis based on the single-photon-counting technique, the model response function $G(t)$ is the theoretical impulse decay function $I(t)$ convoluted with instrument response function $R(t)$.

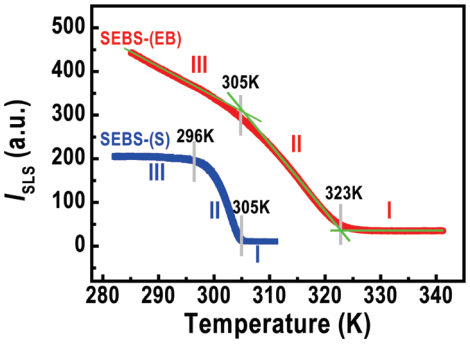

Figure 1. Temperature dependence of SLS intensity (I_{SLS}) at 90° for (a) SEBS-(S) and (b) SEBS-(EB) solutions upon cooling.

Results and Discussion

Temperature Dependence of SLS Intensity of SEBS Solution. As one of the most conventional ways, SLS was used to study the association behavior in solution. Figure 1 plots the temperature dependence of SLS intensity (I_{SLS}) at 90° for SEBS-(S) and SEBS-(EB) solutions upon cooling. Apparently, a dramatic increase in the light scattering intensity (I_{SLS}) can be observed as the temperature is lowered than a certain value, that is, 305 K for SEBS-(S) or 323 K for SEBS-(EB). As known to all, when the ABA-type block copolymer is dissolved in a selective organic solvent, the block copolymer can associate in solution upon cooling to form micelles as a result of different solvation of the copolymer blocks and their incompatibility.[27,28] Thus, the sudden changes in I_{SLS} should result from the appearance of micelles, and the transition temperature can be considered as the critical micelle temperature (T_c).

As shown in Figure 1, in SEBS-(S) solution, I_{SLS} starts to level off at a relatively lower temperature (296 K), which is defined as the equilibrium temperature (T_e), indicating that the equilibrium is overwhelmingly in favor of micelle formation. However, in the case of SEBS-(EB) solution, there is no T_e at low temperature but an inflection temperature (305 K) below which the reduced temperature dependence of I_{SLS} appears. The explanation to this distinct phenomenon should be related to different mechanism and morphologies of micelles formed in two SEBS solutions. It is well-known that, for symmetrical triblock copolymers in selective solvents, the micelles usually consist of two main regions: an inner core containing the insoluble blocks and an outer corona containing both the soluble outer blocks and the solvent molecules.[29] Here, in SEBS-(S) solution, methylene dichloride is a selective solvent for outer blocks (PS). As a consequence, the relatively compact core of micelle formed should be consisting predominantly of insoluble middle blocks (PEB) and surrounded by a swollen protective corona of solvated PS blocks. In most cases, these micelles have spherical shape and a narrow size distribution.[30,31] In contrast, the association in SEBS-(EB) solution would lead to the flowerlike micelles, where the middle block (PEB) forms a loop so that both outer blocks (PS) stay in the micelle core.[32] In this case, however, the existence of gellike networks would also be possible because of a bridging function of the soluble middle blocks extended between the small clusters formed by the outer blocks.[33] In conclusion, the increase of I_{SLS} below 305 K in SEBS-(EB) solution, shown in Figure 1, may be ascribed to the further aggregation between micelles induced by the bridging effect.

Temperature Dependence of DLS of SEBS Solution. To get more extensive information on the aggregate system studied, DLS measurements were also carried out. Figure 2 shows that the scattering vector (q) dependence of average characteristic line width ($\langle\Gamma\rangle$) of SEBS(S) solution at 306 K. It can be seen

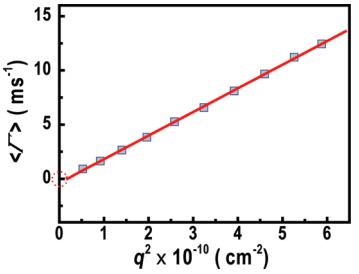

Figure 2. Scattering vector (q) dependence of average characteristic line width ($\langle\Gamma\rangle$) of SEBS(S) solution at 306 K.

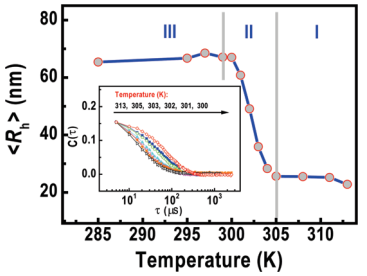

Figure 3. Temperature dependence of hydrodynamic radius, $\langle R_h\rangle$, for SEBS-(EB) solution measured by dynamic light scattering upon cooling. Inset shows the typical intensity−intensity time correlation functions at different temperatures.

that $\langle\Gamma\rangle$ is a linear function of q^2, and the fitted line almost passes through the origin as $q \rightarrow 0$ (with an ignorable deviation). This behavior should be considered as a characteristic of diffusive relaxation.[34]

In the analysis of the DLS data, results based on a cumulant analysis can cause an ill-posed problem unless it is completely fitted to a single-exponential function. Here, as shown in the inset of Figure 3, only one relaxation mode is observed in SEBS(S) solution over the entire temperature range, suggesting micelles are almost formed homogenously. Figure 3 shows the temperature dependence of hydrodynamic radius, $\langle R_h\rangle$, for SEBS-(S) solution upon cooling. Clearly, $\langle R_h\rangle$ first increase sharply below 305 K, suggesting the interchain aggregation, and then levels off below 299 K, representing the finish of the micellization. This result consists well with that obtained with SLS method (see Figure 1). However, in the case of SEBS-(EB) solution, nearly five regimes can be found in the plot of $\langle R_h\rangle$ vs temperature upon cooling, shown in Figure 4. It is worth mentioning that, the correlation function is not a single mode in regimes IV and V (see the inset of Figure 4) so that the values of $\langle R_h\rangle$ in these regimes only reflect the apparent effective radius. In spite of this, the change of $\langle R_h\rangle$ in Figure 4 can be still rationalized as follows: (i) At high temperature (regime I), only free SEBS chains exist in the solution so that $\langle R_h\rangle$ appears to be relatively constant. (ii) As the temperature decreases below 326 K (regime II), $\langle R_h\rangle$ increases with decreasing temperature and the $\langle R_h\rangle$ value is increased to 55 nm, which suggests the aggregation of PS blocks into the cores of flowerlike micelles. It was reported in a previous study that, in *n*-octane/4-methyl-2-pentanone (a selective solvent for PEB blocks), $\langle R_h\rangle$ values of micelles are ~47 nm,[33] which is close to our result. (iii) Subsequently, when the temperature is lower than 317 K (regime III), $\langle R_h\rangle$ increases slightly with the temperature decreases. This phenomenon implies that the system may reach a relative equilibrium state, in which all SEBS chains have aggregated into micelles. Usually, there are two types of possible structures for association particles of ABA triblock copolymers when the solvent is selectively good for B block.

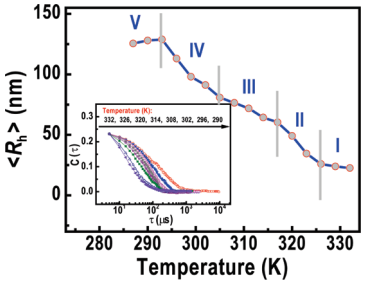

Figure 4. Temperature dependence of hydrodynamic radius, $\langle R_h\rangle$, for SEBS-(EB) solution measured by dynamic light scattering upon cooling. Inset shows the typical intensity−intensity time correlation functions at different temperatures.

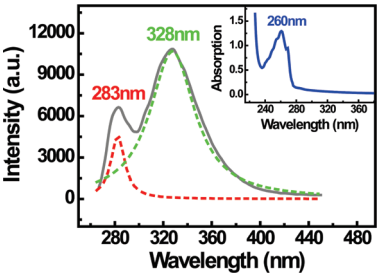

Figure 5. Steady-state intrinsic fluorescence spectra of SEBS-(S) solution at 300 K (λ_{ex} = 260 nm). The inset shows the UV/vis absorption spectrum.

One is a well-defined flowerlike micelle formed by a close association of all A blocks inside the core−shell-like micelle, while another involves intermicelle aggregate in which the two A blocks of a copolymer chain insert into two different micelles to form a bridge.[35,36] On the basis of this idea, regime III can be regarded as an induction period for the intermicellar aggregation. (iv) As the temperature decreases further (regime IV), $\langle R_h\rangle$ increases considerably again upon cooling below 303 K, which should be ascribed to the aggregation between different SEBS micelles due to the dangling PS end. (v) Finally, when the temperature is below 292 K (regime IV), the micellization process comes to a point of completion.

Intrinsic Fluorescence of SEBS-(S) Solution. Since it has been proven that the fluorimetry can provide highly localized information,[37] to further understand our results obtained above, Figure 5 shows the steady-state intrinsic fluorescence spectra of SEBS-(S) solution at a concentration of 1.2×10^{-3} g/mL (λ_{ex} = 260 nm). As expected, a maximum intensity can be observed at 328 nm, with a second, lesser peak at 283 nm, which should be attributed to excimer and monomer fluorescence of PS block, respectively. The former is due to emission from an excited-state dimer consisting of two phenyl rings in a parallel, sandwich-like conformation[38−40] while the latter is due to emission from a single excited-state phenyl ring.

It should be noted that there exist two types of nominal excimer forming site: (i) intermolecular interaction between rings on different chains and (ii) intramolecular interaction between phenyl rings on adjacent and/or nonadjacent chain segments.[41−43] Here, the overlap concentration (C^*) of SEBS chain was evaluated to be 4×10^{-2} g/mL according to

$$C^* = \frac{3M_w}{4\pi N_A R_g{}^3} \quad (1)$$

where M_w, N_A, and R_g are weight-average molecular weight, Avogadro constant, and the radius of gyration, respectively.[44] Clearly, the concentration used in our experiment

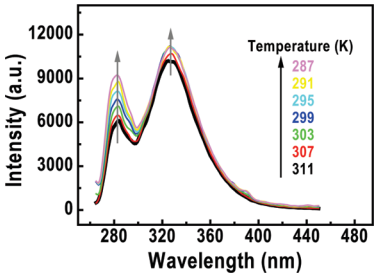

Figure 6. Steady-state intrinsic fluorescence spectra of SEBS-(S) solution during cooling. The thickest line indicates the spectrum at 311 K.

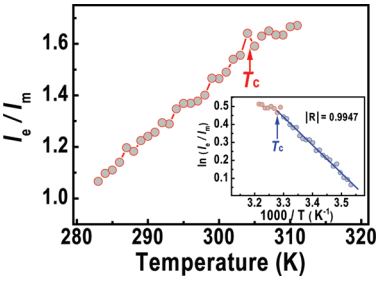

Figure 7. Temperature dependence of I_e/I_m for SEBS-(S) solution upon cooling. The inset shows the Arrhenius plot of $\ln(I_e/I_m)$.

($C = 1.2 \times 10^{-3}$ g/mL) is much lower than this overlap concentration. Polymer chains are thus far apart, and intermolecular interaction is very weak. In this context, the fluorescence emission at 328 nm should be mainly originated from intramolecular excimers. In order to eliminate the interference of adjacent peaks and obtain the accurate value of fluorescence intensity, the deconvolution treatment of these peaks is necessary and accomplished by fitting with a Gaussian distribution mode. In the following sections, the intensities of fitted fluorescence peaks for monomer and excimer will be referred to as I_m and I_e, respectively.

Figure 6 illustrates the steady-state intrinsic fluorescence spectra of SEBS-(S) solution upon cooling from 311 to 287 K (only spectra at every 4 K internal were shown for clarity). It can be seen that the intensity increases with the temperature decreases, suggesting the sensitivity of intrinsic fluorescence in following this aggregation process. Fundamentally, the change in fluorescence intensity can be induced by several complex factors, e.g., the refraction index, nonradiative and radiative energy transfer rates.[45,46] Thus, we have chosen not to use the temperature dependence of the maximum emission intensity to monitor the macromolecular motions of SEBS chains. Instead, we employed the excimer-to-monomer intensity ratio (I_e/I_m) because the excimer is only formed when aromatic rings closely approach each other within 3−4 Å; that is, they are quite sensitive to the formation of small aggregates containing two or more aromatic groups and their compactness, with the latter determining the mobility of aromatic groups and their encounter probability.[47−49]

As shown in Figure 7, the value of I_e/I_m first slightly decreases at $T > T_c$ (~305 K) and then dramatically decreases with the decreasing temperature at $T < T_c$. Before we present the interpretation of this result, it is necessary to review briefly several aspects of the photophysics of the aromatic vinyl polymers. Usually, I_e/I_m depends upon three major factors:[41−43] (i) The electronic stability of the excimer complex, as manifested through the radiative and nonradiative fluorescence decay constants of the excimer and monomer. These photophysical parameters should reflect very short-range interactions between the excimer complex on polymer chains and

Scheme 2. Kinetic Scheme for Fluorescence Decay of Monomer and Excimer

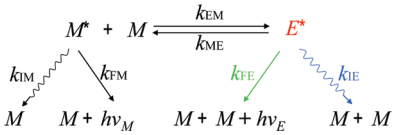

the local environment in the solution. (ii) The extent to which the efficiency of the exciton migration depends upon the conformational structure of polymer chain. In general, the direct absorption of incident radiation is insignificant due to the small number of excimer-forming sites, and the most common situation is that an isolated aromatic ring absorbs a photon of incident radiation followed by a rapid migration of the excitation until competitive trapping occurs at an excimer site. (iii) The number and type of excimer-forming site. The intramolecular site can provide information on the conformational statistics of the polymer chains and should be sensitive to chain coiling and, thus, to thermodynamic interaction between blocks in the copolymer where excimer can be formed in one of the blocks. Besides, the intermolecular site formed between aromatic rings on different polymer chains should also be sensitive to the thermodynamics in polymer blends where one of components produces excimer. More specifically, the number of intermolecular sites should increase with the degree of chain aggregation in the solution.

To quantitatively describe the above factors, the Birks scheme is taken into consideration here. As shown in Scheme 2,[45] the encounter of an excited monomer (M*) with a nonexcited monomer (M) can lead to the formation of an excimer (E*) with a rate constant k_{EM}. At the same time, M* can also radiatively (k_{FM}) or nonradiatively (k_{IM}) deactivate to the ground state. Similarly, E* can not only dissociate to give M* and M with a rate constant k_{ME} but also radiatively (k_{FE}) and nonradiatively (k_{IE}) deactivate to the ground state, giving rise to two monomer units. Under photostationary conditions, this scheme provides the ratio of excimer-to-monomer fluorescence intensities:

$$\frac{I_e}{I_m} \propto \frac{k_{EM}}{k_{FE} + k_{IE} + k_{ME}} \tag{2}$$

In general, formation and dissociation of an excimer in solution occur in two temperature ranges:[50,51] (i) in low-temperature limit (LTL), the formation of an excimer is diffusion-controlled, and the higher temperature will reduce the viscosity and favor the formation of excimers; (ii) in high-temperature limit (HTL), from the thermodynamic point of view, the increase in temperature will attenuate the van der Waals interaction and favor the dissociation of excimers. The Stevens−Ban plot shows that the measurement of the ratio also allows for the calculation of some parameters for excimer formation according to the Arrhenius equation:[52]

$$\frac{\mathrm{d}\ln(I_e/I_m)}{\mathrm{d}(1/T)} = -\frac{E_a^a - E_a^d}{R} = -\frac{\Delta H}{R} \tag{3}$$

where E_a^a and E_a^d are the activation energies for excimer association and dissociation, respectively, and ΔH reflects the enthalpy of formation or the binding energy. The resulting Arrhenius plot of $\ln(I_e/I_m)$ for SEBS-(S) solution is presented in the inset of Figure 7, and $\Delta H = 12.95$ kJ/mol is determined from the slope of best-fit line at $T < T_c$.

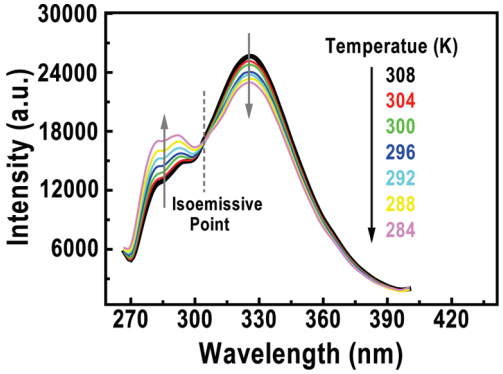

Figure 8. Steady-state intrinsic fluorescence spectra of PS/methylene dichloride solution during cooling. The thickest line indicates the spectrum at 308 K.

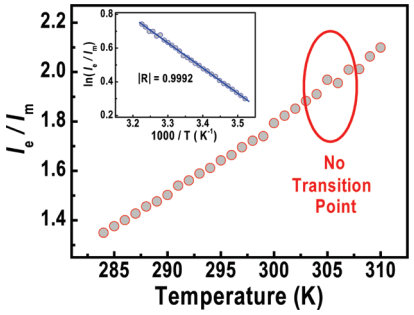

Figure 9. Temperature dependence of I_e/I_m for pure PS in methylene dichloride upon cooling. The inset shows the Arrhenius plot of $\ln(I_e/I_m)$.

To verify the above results, the temperature-dependent fluorescence spectra of pure PS in methylene dichloride with the identical phenyl group concentration were measured, shown in Figure 8. On controlled cooling, the monomer emission increases while excimer emission decreases, leading to a clear isoemissive point at 304 nm, which suggests that the rate parameters for the nonradiative relaxation of the monomer and excimer are independent of temperature over the temperature range studied here.[53] More importantly, this phenomenon implies that the energy migration of excimer in pure PS solution should be different from that in SEBS-(S) solution due to the existence of PEB block. Moreover, as shown in Figure 9, the monotonous decrease in the value of I_e/I_m upon cooling suggests that the temperature range studied here (284−310 K) is in LTL of PS excimer where the formation of an excimer is diffusion-controlled and the excimer dissociation rate constant is ignorable ($k_{ME} \ll k_{FE} + k_{IE}$).[54] Note that, in the inset of Figure 7, there is no inflection point at around 305 K, and the value of $\ln(I_e/I_m)$ is a strictly linear function of $1/T$, indicating that a deviation of Stevens−Ban plot in Figure 7 should be induced by a phase transition in SEBS(S) solution.

In order to get a comprehensive understanding of the conformational transition of SEBS chain, it is necessary to analyze the change of each rate constant shown in eq 2. For a diffusion-controlled system, Cuniberti and Perico[55] have found that the rate constant k_{EM} should be concentration dependent, that is

$$k_{EM} \propto k_{diff}[M]_{eff} \tag{4}$$

where the rate constant k_{diff} describes the effective molecular diffusion of the segments bearing the reacting labels and $[M]_{eff}$ represents the effective concentration of the unexcited chromophores in the neighborhood of the excited species. Since the excited excimer lifetime is defined by

$$\tau_e = \frac{1}{k_{FE} + k_{IE} + k_{ME}} \tag{5}$$

Thus, the eq 2 can be rewritten as

$$\frac{I_e}{I_m} \propto k_{diff}[M]_{eff}\tau_e \tag{6}$$

Clearly, three parameters need to be considered. k_{diff} is inversely proportional to viscosity and decreases with increased rigidity of the medium. So it is easy to understand that k_{diff} decreases with the decreasing temperature. However, the evaluation of $[M]_{eff}$ is much more complicated than expected since it depends on both the type of excimer-forming site (interchain or intrachain) and the conformation of the chain (expanded or collapsed). This issue should be clearer when τ_e is determined because the transient-state fluorescence data can reflect some information related to conformational transition. Thus, the detailed analysis of the fluorescence decay will be given below.

Essentially, the transient-state fluorescence is much more sensitive than the steady-state fluorescence. To deduct any contribution from monomer emission, it is necessary to strictly distinguish the fluorescence emission between excimer and monomer. Therefore, in time-resolved fluorescence analysis, one cannot rely on the emission boundary between excimer and monomer determined by the deconvolution treatment of adjacent steady-state fluorescence peaks. Instead, we should analyze the variance of fluorescence decays from the onset to tail of the emission band (see Figure 1S). To obtain a more specific results, all the decays were intendedly fitted by biexponential functions, as reflected by the goodness-of-fit parameter $\chi^2 = 1.03 \pm 0.01$, and two important parameters, i.e., the fluorescence lifetime (τ_i) and the corresponding pre-exponential factors (α_i), were determined directly. As shown in Figure 10a, both short and long lifetimes (τ_1 and τ_2) increase with the increasing wavelength, which reflects the contribution of monomer to excimer varies with emission wavelengths. In addition, it is clear in Figure 10b that the pre-exponential factor for short lifetime (α_1) is dominant at wavelengths below 280 nm, while the pre-exponential factor for long lifetime (α_2) is dominant at wavelengths above 330 nm. Since the monomer and excimer emission peaks are located at 283 and 328 nm, respectively (see Figure 5), the result in Figure 10a,b suggests the short lifetime at shorter wavelengths ($\tau_1 \approx 1$ ns) is associated with the decay time of the monomer while the long lifetime at longer wavelengths ($\tau_2 \approx 11$ ns) is associated with the decay time of the excimer. These assignments are very similar to the lifetimes of monomer (1.1 ± 0.3 ns) and excimer (12.5 ± 1 ns) of polystyrene in fluid solution.[56]

Also, the fractional contribution (f_i) is determined by[57]

$$f_i = \frac{\alpha_i\tau_i}{\sum_j \alpha_j\tau_j} \tag{7}$$

Because the term $\alpha_i\tau_i$ is proportional to the area under the decay curve for each decay time, it is understandable that only one decay component contributes to steady-state fluorescence emission when $f = 1$. As can be seen in Figure 10c, the fractional contribution of excimer (f_2) is equal to 1 at the wavelengths longer than 345 nm, suggesting that there is not any contribution from monomer emission in this wavelength range. To better analyze the time-resolved fluorescence data of excimer of SEBS, our attention is only focused on the emission wavelength at 345 nm in the following sections.

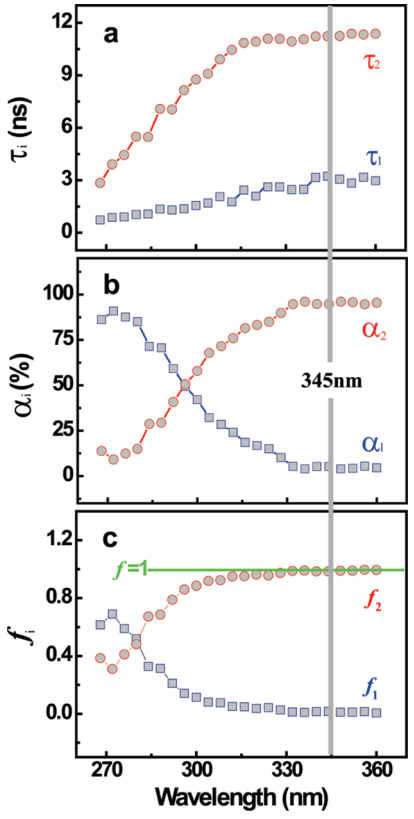

Figure 10. Emission wavelength dependence of (a) fluorescence decay lifetimes (τ_i), (b) pre-exponential factors (α_i), and (c) fractional contributions (f_i) for SEBS-(S) solution (λ_{ex} = 260 nm).

All the intrinsic fluorescence decay profiles for SEBS-(S) solution at various temperatures upon cooling can be best fitted by the single-exponential function ($\chi^2 = 1.03 \pm 0.01$) (see Figure 2S). Generally, the intrinsic excimer lifetime, $\Gamma_e = 1/(k_{FE} + k_{IE})$, increases with the decreasing temperature.[58,59] Since the temperature ranges applied for pure PS and SEBS(S) solution are identical and k_{ME} is neglectable in LTL, if the energy migrations of excimers in these two systems are similar, the excimer lifetime (τ_e) should be also expected to increase upon cooling. Figure 11 shows the temperature dependence of τ_e. Unexpectedly, τ_e decreases with the temperature decreases. This discrepancy not only confirms again the difference of excimer formation kinetics between pure PS and SEBS(S) solution but also demonstrates that k_{EM} is the predominant rate constant ($k_{ME} \gg k_{FE} + k_{IE}$) and dramatically increases with the temperature decreases. Birks et al. found that, for excimer fluorescence in small molecules, the rise in temperature would dramatically enhance the molecular motions that distorted the symmetrical parallel sandwich excimer configuration and lead to the increased intermolecular vibrational interaction and consequently result in the decrease of excimer lifetime.[60] From this result, it is reasonable to infer that the lifetime of excimer may be directly affected by the stability of the symmetrical parallel sandwich configuration. In other words, the easier the configuration is distorted, the shorter the lifetime. Herein, the chromophores (benzene rings) are completely located on the SEBS chains, and once the excimer is formed, the motions of benzene rings are restricted by the macromolecular chains. Thus, conceivably, the stability of excimer of SEBS should depend on the degree of extension of polymer chains. The stretched polymer chains can not only increase the intermolecular distance of benzene rings, hence lowering the probability of excimer formation, but also expose

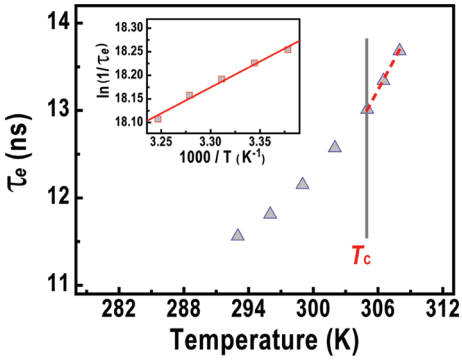

Figure 11. Temperature dependence of the excimer lifetime (τ_e) for SEBS-(S) solution upon cooling. The inset shows the Arrhenius plot of $1/\tau_e$.

the excimer to more solvent molecules, which makes it easier to break the parallel sandwich configuration and thus raise the excimer association rate k_{EM}. As a consequence, the decrease of τ_e in Figure 11 reveals that the PS block adopted a more extended configuration during the micellization of SEBS-(S) solution.

However, it is worth mentioning that the reduction in τ_e upon cooling can be also observed at both $T > 305$ K and $T < 296$ K. As shown in SLS data (see Figure 1), the micellization process almost occurs at 305 K and completes at 296 K; thus, the possible answer to this change of τ_e should be based on the fact that (i) PEB block initiates to shrink due to its decreased solubility of PEB block once the reduction of temperature occurs even before the micellization, which pulls the adjacent PS segments into a stretched conformation, and (ii) outer blocks (PS) can be further stretched due to the contraction of middle block (PEB) upon further cooling when the equilibrium in solution is overwhelmingly in favor of micelle formation. The further contraction of micelle can be also supported by a careful observation of the slight decrease in micelle size at $T < 296$ K, shown in DLS data (see Figure 3). Besides, it was also demonstrated by SANS that the micelles of ABA copolymer would carry less solvent molecules and become more compact at the late stage of micellization process.[12] Thus, the above results also suggest that the fluorescence measurement is a very sensitive method and can offer us the information on a scale smaller than SLS.

To further describe the chain aggregation in SEBS-(S) solution, the activation energy of excimer association $E_a^d = -9.09$ kJ/mol can be estimated in the Arrhenius plot of excimer lifetime according to eqs 2, 3, and 5, shown in the inset of Figure 9. Besides, the activation energy for excimer formation $E_a^a = 3.86$ kJ/mol can be also easily determined by substituting the values of ΔH and E_a^d into eq 3.

Hence, both k_{diff} and τ_e are clear now. Let us go back to discuss the change of $[M]_{eff}$ during the micellization process. On one hand, according to the results obtained in pure PS/methylene dichloride solution (see Figure 8), we have found that the change of k_{diff} cannot lead to an inflection point in the plot of I_e/I_m versus temperature in the whole temperature range we studied when $[M]_{eff}$ is considered as a constant in the absence of the phase transition. On the other hand, τ_e almost decreases linearly with the temperature decreases. Thus, according to eq 6, it is reasonable to infer that there should be an inflection point for the variance of $[M]_{eff}$ at around T_c. At temperature above T_c, only intrachain excimers exist in SEBS-(S) solution, and the chain segments in PS block are more and more stretched upon cooling, which means $[M]_{eff}$ decreases with the decreasing temperature before micellization. Understandably, the apart chain can encounter and

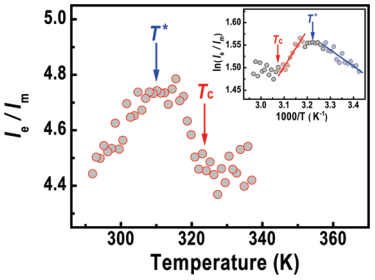

Figure 12. Temperature dependence of the excimer-to-monomer fluorescence ratio (I_e/I_m) for SEBS-(EB) solution upon cooling. The inset shows the Arrhenius plot of $\ln(I_e/I_m)$.

produce excimer intramolecularly during micellization, which would bring out a sharp rise of $[M]_{eff}$. However, $[M]_{eff}$ should decrease more drastically at temperatures below T_c to allow for the appearance of an inflection point. This strongly suggests that the dominant excimers in SEBS micelles must not be interchain but intrachain ones so that $[M]_{eff}$ can be greatly reduced by the chain stretching. Generally, to interpret this interesting result, the exact dimension of core and shell should be necessary. Because of lack of SANS data, only a rough estimate is given here. It was recently demonstrated by Ogata et al. that in *N*-methylpyrrolidone (a selective solvent for PS block) the formed SEBS core−shell micelle is composed of 65 polymer chains, with a highly dense PEB core (radius R_c = 4.5 nm) and thick PS shell (thickness R_s = 22.9 nm).[61] According to these data, the average interchain distance d can be easily estimated to range from 22 Å (at the core surface) to 114 Å (at the surface of the corona), assuming that SEBS chains were distributed evenly in a micelle. Apparently, this value is much greater than the required inter-ring distance (3−4 Å) of the excimer. In addition, in our case, due to less polarity of the solvent used, the micelle is expected to be less compact than that in *N*-methylpyrrolidone, resulting in a larger d and lower possibility of interchain excimer formation.

Intrinsic Fluorescence of SEBS-(EB) Solution. Similar analysis was done of the temperature dependence of I_e/I_m of SEBS-(EB) solution shown in Figure 12. As mentioned above, the transition temperature T_c obtained in the SLS method is located at 323 K (see Figure 1). Here, the value of I_e/I_m first decreases slightly at $T > T_c$ and then rises continuously at $T < T_c$ with decreasing temperature. Finally, an abrupt reduction of I_e/I_m can be observed on further cooling when temperature is lowered to a turnover point T^* (~310 K). Since (i) k_{diff} decreases with decreasing temperature and (ii) τ_e usually varies monotonously with the temperature which will be mentioned in detailed later, the data shown in Figure 11 can be rationalized as follows. As the temperature decreases below T_c (323 K), the solvent becomes bad for PS block and the phenyl rings get closer to each other so that $[M]_{eff}$ dramatically increases and I_e/I_m rises with decreasing temperature. The increase in $[M]_{eff}$ cannot be balanced by the decrease in k_{diff}, and the change of τ_e until the temperature is decreased to T^* (310 K) where a small plateau can be observed. Note that, in the light scattering results (Figures 1 and 4), further aggregation between micelles can occur in SEBS-(EB) solution. Thus, the decrease in I_e/I_m below T^* also implies that the intermicellar aggregation will not lead to a dramatic decrease in interchain distance of PS block. From the slope of Arrhenius plot in the inset of Figure 12, the binding energy ΔH at $T^* < T < T_c$ and $T < T^*$ can be determined to be −3.0 and 6.7 kJ/mol, respectively.

To further study the conformational change of macromolecular chain in SEBS-(EB) solution, the excimer fluorescence decay was also studied at various temperatures upon cooling

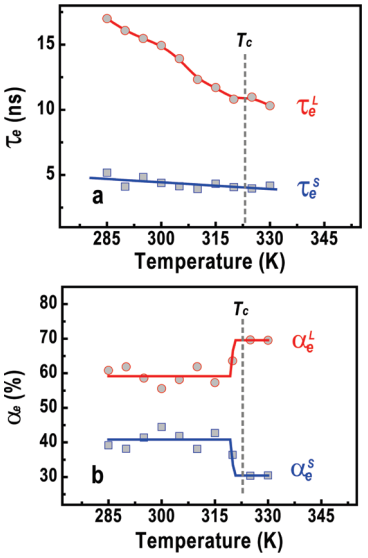

Figure 13. Temperature dependence of (a) lifetime τ_e and (b) preexponential factor α_e of excimer in SEBS-(EB) solution upon cooling.

(see Figure 3S). Surprisingly, in this case, all decays are not monoexponential but biexponential ($\chi^2 = 1.04 \pm 0.01$), which strongly suggests the existence of two distinct relaxation processes of excimer. As can be seen in Figure 13a, the value of long lifetime component (τ_e^L) is almost twice longer than that of short lifetime component (τ_e^S) at $T > T_c$. These two lifetimes should not be associated with intra- and intermolecular excimer, respectively, because the excimer lifetime is not significantly affected by the mode (intra vs inter) of formation.[59] Thus, the excimer lifetimes most probably depends on the chain flexibility of each block and/or the degree of solvent selectivity. The conformation of hard block (PS block) is complete homogeneous in its good solvent but microheterogenous if the solvent is selective for the soft block connected with it (PEB block). Generally, the two different lifetimes in SEBS-(EB) solution should be associated with different part of the PS block. In this case, PEB block forms open, extended structure while PS block is relatively collapsed due to the effective self-affinity of the polymer chain. It is understandable that the motion of PEB segment could give rise to the stretching of some PS segment to some extent via the chemical joint of two blocks. As a consequence, on the basis of the foregoing analysis on lifetime, τ_e^S and τ_e^L are assigned to the emission of the PS segment adjacent and nonadjacent to PEB block, respectively.

As can be seen in Figure 13a, τ_e^L increases with decreasing temperature while the change of τ_e^S is nearly negligible. Here, it is difficult for us to resolve, with confidence, the contribution of conformational change of polymer chain, since the k_{IE} and k_{FE} also contribute to the increase of lifetime values upon cooling. Even so, there are still some further conclusions that can be made. In SEBS-(EB) solution, the micellization process can considerably affect the conformation of the PS segment nonadjacent to PEB block but have little effect on that adjacent to PEB block.

Conclusions

In this work, the aggregation behaviors of SEBS were investigated in selective solvent for PS block (methylene dichloride) and PEB block (mixture of *n*-hexane and cyclohexane), i.e., SEBS-(S) and SEBS-(EB) solution, respectively. Both SLS and DLS showed that the conformational change of molecular chain underwent three stages in SEBS-(S) solution. The fluorescence analysis

suggested that (i) above T_c, PEB block initiated to slightly shrink upon cooling which pulled the adjacent PS segments into a stretched conformation; (ii) when the micellization process occurred, PS segments was further stretched during the aggregation of PEB block into micelle cores, resulting in the great decrease in the amount of intramolecular excimers. However, for SEBS-(EB) solution, five stages were observed in DLS result due to the different aggregation mechanism during the micellization. In this case, the further aggregation between micelles was induced by the bridging effect of the dangling outer block (PS). The steady-state fluorescence results indicated that the intermicellar aggregation would not lead to a dramatic decrease in interchain distance of PS block in micelle cores. Besides, the time-resolved fluorescence results revealed that the excimer decay was monoexponential in SEBS-(S) solution but biexponential in SEBS-(EB) solution, suggesting that the conformation of PS block was completely homogeneous in its selective solvent but microheterogeneous in the solvent selective for PEB block. The temperature dependence of lifetime showed that the micellization process of SEBS-(EB) solution can considerably affect the conformation of the PS segment nonadjacent to PEB block but have little effect on that adjacent to PEB block. It is believed that this work may bring out the new development to the interpretation and full understanding of aggregation behavior of ABA block copolymer in selective solvents.

Acknowledgment. X. D. Chen acknowledges the financial support from the program of National Natural Science Foundation of China (Grants 50973129 and 50673101), Natural Science Foundation of Guangdong province (Grant 07003702), and China Postdoctoral Science Foundation (Grant 20100470953).

Supporting Information Available: Figures 1S−3S. This material is available free of charge via the Internet at http://pubs.acs.org.

References and Notes

(1) Balsara, N. P.; Tirrell, M.; Lodge, T. P. *Macromolecules* **1991**, *24*, 1975.
(2) Zhou, Z.; Chu, B. *Macromolecules* **1994**, *27*, 2025.
(3) Raspaud, E.; Lairez, D.; Adam, M.; Carton, J.-P. *Macromolecules* **1994**, *27*, 2956.
(4) Zhou, Z.; Chu, B.; Peiffer, D. G. *Langmuir* **1995**, *11*, 1956.
(5) Tuzar, Z.; Kratochvil, P. In *Surface and Colloid Science*; Matigevic, E., Ed.; Plenum Press: New York, 1993.
(6) Liu, S.; Weaver, J. V. M.; Tang, Y.; Billingham, N. C.; Armes, S. P. *Macromolecules* **2002**, *35*, 6121.
(7) Zheng, P.; Jiang, X.; Zhang, X.; Zhang, W.; Shi, L. *Langmuir* **2006**, *22*, 9393.
(8) Li, Y.; Lokitz, B. S.; McCormick, C. L. *Macromolecules* **2006**, *39*, 81.
(9) Kumbhakar, M.; Ganguly, R. *J. Phys. Chem. B* **2007**, *111*, 3935.
(10) Zhang, W. Z.; Chen, X. D.; Luo, W.; Yang, J.; Zhang, M. Q.; Zhu, F. M. *Macromolecules* **2009**, *42*, 1720.
(11) Zhu, P. W.; Napper, D. H. *Macromolecules* **1999**, *32*, 2068.
(12) Liu, Y.; Chen, S.; Huang, J. S. *Macromolecules* **1998**, *31*, 2236.
(13) Lopffer, M.; Bokobza, L.; Monnerie, L. *Macromolecules* **1998**, *31*, 8291.
(14) Moffitt, M.; Farinha, J. P. S.; Winnik, M. A.; Rohr, U.; Muellen, K. *Macromolecules* **1999**, *32*, 4895.
(15) Corrales, T.; Peinado, C.; Bosch, P.; Catalina, F. *Polymer* **2004**, *45*, 1545.
(16) Halary, J. L.; Ubrich, J. M.; Monnerie, L.; Yang, H.; Stein, R. S. *Polym. Commun.* **1985**, *26*, 73.
(17) Zhang, M. Q. *Exp. Polym. Lett.* **2008**, *2*, 835.
(18) Tsai, F. J.; Torkelson, J. M. *Macromolecules* **1988**, *21*, 1026.
(19) Clauss, B.; Salem, D. R. *Macromolecules* **1995**, *28*, 8328.
(20) Ylitalo, D. A.; Frank, C. W. *Polymer* **1996**, *37*, 4969.
(21) Sanz, A.; Mendicuti, F. *Polymer* **2002**, *43*, 6123.
(22) Luo, W.; Liao, Z.; Yang, J.; Li, Y.; Chen, X.; Mai, K.; Zhang, M. *Macromolecules* **2008**, *41*, 7513.
(23) Luo, W.; Chen, Y.; Chen, X.; Liao, Z.; Mai, K.; Zhang, M. *Macromolecules* **2008**, *41*, 3912.
(24) Quintana, J. R.; Janez, M. D.; Hernaez, E.; Garcıa, A.; Katime, I. *Macromolecules* **1998**, *31*, 6865.
(25) Wu, C.; Woo, K.; Jiang, M. *Macromolecules* **1996**, *29*, 5361.
(26) Ovejero, G.; Perez, P.; Romero, M. D.; Guzman, I.; Diez, E. *Eur. Polym. J.* **2007**, *43*, 1444.
(27) Quintana, J. R.; Villacampa, M.; Katime, I. *Rev. Zberoam. Pollm.* **1992**, *1*, 5.
(28) Price, C. *Pure Appl. Chem.* **1983**, *55*, 1563.
(29) Quintana, J. R.; Villacampa, M.; Katime, I. In *The Polymeric Materials Encyclopedia. Synthesis, Properties and Applications*; Salamone, J. C., Ed.; CRC Press: Boca Raton, FL, 1996.
(30) Brown, R. A.; Masters, A. J.; Price, C.; Yuan, X. F. *Comprehesive Polymer Science*; Booth, C., Price, C., Eds.; Pergamon Press: Oxford, 1989.
(31) Villacampa, M.; Quintana, J. R.; Salazar, R.; Katime, I. *Macromolecules* **1995**, *28*, 1025.
(32) Quintana, J. R.; Janez, M. D.; Katime, I. *Langmuir* **1997**, *13*, 2640.
(33) Quintana, J. R.; Hernaez, E.; Inchausti, I.; Katime, I. *J. Phys. Chem. B* **2000**, *104*, 1439.
(34) Brown, W.; Štěpánek, P. *Macromolecules* **1991**, *24*, 5484.
(35) Zhou, Z.; Chu, B.; Nace, V. M.; Yang, Y.-W.; Booth, C. *Macromolecules* **1996**, *29*, 3663.
(36) Martini, L.; Attwood, D.; Collett, J. H.; Nicholas, C. V.; Tandekaew, S.; Deng, N. J.; Heatley, F.; Booth, C. *J. Chem. Soc., Faraday Trans.* **1994**, *90*, 1961.
(37) Larbi, F. B. C.; Halary, J. L.; Monnerie, L. *Macromolecules* **1991**, *24*, 867.
(38) Vala, M. T.; Haebig, J.; Rice, S. A. *J. Chem. Phys.* **1965**, *43*, 886.
(39) TorkelSon, J. M.; Lipsky, S.; Tirrell, M. *Macromolecules* **1981**, *14*, 1601.
(40) TorkelSon, J. M.; Lipsky, S.; Tirrell, M.; Tirrell, D. A. *Macromolecules* **1983**, *16*, 326.
(41) Frank, C. W.; Harrah, L. A. *J. Chem. Phys.* **1974**, *61*, 1526.
(42) Frank, C. W. *J. Chem. Phys.* **1974**, *61*, 2015.
(43) Frank, C. W. *Macromolecules* **1975**, *8*, 305.
(44) Teraoka, I. *Polymer Solutions*; John Wiley & Sons: New York, 2002.
(45) Birks, J. B. *Photophysics of Aromatics Molecules*; Wiley: New York, 1970.
(46) Beaucage, G.; Composto, R.; Stein, R. S. *J. Polym. Sci., Polym. Phys.* **1993**, *31*, 319.
(47) Picarra, S.; Relogio, P.; Afonso, C. A. M.; Martinho, J. M. G.; Farinha, J. P. S. *Macromolecules* **2004**, *37*, 1670–1670.
(48) Farinha, J. P. S.; Picarra, S.; Miesel, K.; Martinho, J. M. G. *J. Phys. Chem. B* **2001**, *105*, 10536.
(49) Winnik, F. M. *Macromolecules* **1990**, *23*, 1647.
(50) Klöpffer, W. *Organic Molecular Photophysics*; Wiley: London, 1973; Vol. *1*, p 357.
(51) Forster, T. *Angew. Chem., Int. Ed.* **1969**, *8*, 333.
(52) Stevens, B.; Ban, M. I. *Trans. Faraday Soc.* **1964**, *60*, 1515.
(53) Hamilton, T. D. S.; Naqvi, K. R. *Chem. Phys. Lett.* **1968**, *2*, 374.
(54) Seixas de Melo, J.; Pina, J.; Lodeiro, C.; Parola, A. J.; Lima, J. C.; Albelda, M. T.; Clares, M. P.; Garcia-Espana, E.; Soriano, C. *J. Phys. Chem. A* **2003**, *107*, 11307.
(55) Cuniberti, C.; Perico, A. *Eur. Polym. J.* **1980**, *16*, 887–893.
(56) Gupta, M. C.; Gupta, A.; Horwitz, J.; Kliger, D. *Macromolecules* **1982**, *15*, 1372.
(57) Lakowicz, J. R. *Principles of Fluorescence Spectroscopy*, 3rd ed.; Springer: New York, 2006.
(58) Martinho, J. M. G.; Farinha, J. P.; Berberan-Santos, M. N.; Duhamel, J.; Winnik, M. A. *J. Chem. Phys.* **1992**, *96*, 8143.
(59) Semerak, S. N.; Frank, C. W. *Adv. Polym. Sci.* **1984**, *54*, 31.
(60) Birks, J. B.; Alwattar, A. J. H.; Lumb, M. D. *Chem. Phys. Lett.* **1971**, *11*, 89.
(61) Ogata, Y.; Mogi, T.; Makita, Y. *J. Polym. Sci., Polym. Phys.* **2010**, *48*, 588.